Effects of combining flow intermittency and exposure to emerging contaminants on the composition and metabolic response of streambed biofilm bacterial communities

Marko Rožman[1,2*], Itziar Lekunberri[2], Ivana Grgić[1], Carles M. Borrego[2,4], Mira Petrović[2,3]

[1] Ruđer Bošković Institute, Bijenička cesta 54, 10000 Zagreb, Croatia

[2] Catalan Institute for Water Research (ICRA), Emili Grahit 101, 17003 Girona, Spain

[3] University of Girona, E-17003 Girona, Spain

[4] Group of Molecular Microbial Ecology, Institute of Aquatic Ecology, University of Girona, E-17001 Girona, Spain

[*]Corresponding author.

Marko Rožman: marko.rozman@irb.hr

Abstract

Freshwater ecosystems are characterised by the co-occurrence of stressors that simultaneously affect the biota. Among these, flow intermittency and chemical pollution severely impair the diversity and functioning of streambed bacterial communities. Using an artificial streams mesocosm facility, this study examined how desiccation and pollution caused by emerging contaminants affect the composition of stream biofilm bacterial communities, their metabolic profiles, and interactions with their environment. Through integrative analysis of the composition of biofilm communities, characterization of their metabolome and composition of the dissolved organic matter, we found strong genotype-to-phenotype interconnections. The strongest correlation was found between the composition and metabolism of the bacterial community, both of which were influenced by incubation time and desiccation. Unexpectedly, no effect of the emerging contaminants was observed, which was due to the low concentration of the emerging contaminants and the dominant impact of desiccation. However, biofilm bacterial communities modified the chemical composition of their environment under the effect of pollution. Considering the tentatively identified classes of metabolites, we hypothesised that the biofilm response to desiccation was mainly intracellular while the response to chemical pollution was extracellular. The present study demonstrates that metabolite and dissolved organic matter profiling may be effectively integrated with compositional analysis of stream biofilm communities to yield a more complete picture of changes in response to stressors**.**

Keywords: contaminants of emerging concern, streambed biofilms, desiccation, global change, ecosystem services

1. Introduction

Due to various natural and anthropogenic disturbances, surface waters are rarely found in their natural state. Nowadays, freshwater ecosystems are exposed to a combination of both natural (*e.g.*, high temperatures, desiccation) and anthropogenic (*e.g.*, pesticides, pharmaceutical compounds) stressors that alter stream metabolism, its ecological function (Keller et al., 2014; Murray et al., 2010; Sabater et al., 2016) and contribute to the "dark side" of the subsidies (Grgić et al., 2023; Veseli et al., 2022). An important component of freshwater ecosystems are streambed biofilms, which are complex microbial systems that dynamically interact with the environment, exchanging and transforming organic and inorganic compounds, and responding to both physical and chemical factors (Battin et al., 2016). Biofilms thus actively contribute to biogeochemistry of rivers and are at the base of key ecological functions of fluvial ecosystems (Battin et al., 2016). As part of freshwater ecosystems, biofilm communities are often exposed to flow intermittency and the effects of pharmaceutical pollution (Corcoll et al., 2015). There is evidence that flow interruption alters biofilm sensitivity to toxicants (Courcoul et al., 2022; Proia et al., 2013). In addition, several authors have indicated that flow intermittency modulates the effects of contaminants on streambed biofilm communities (Corcoll et al., 2015; Courcoul et al., 2022; Romero et al., 2020; Serra-Compte et al., 2018). Notably, previously dried biofilms showed a lower sensitivity to complex contaminants mixtures than undisturbed biofilms (Corcoll et al., 2015; Courcoul et al., 2022). Such multi-stressor conditions, combining hydrological discontinuities with the presence of contaminants may influence stream metabolism with a tendency to heterotrophy (Calapez et al., 2020; Corcoll et al., 2015; Courcoul et al., 2022). In general, these studies highlight the importance of considering the hydrological history of a biofilm community when assessing its sensitivity to contaminants.

While some of the studies (Calapez et al., 2020; Corcoll et al., 2015; Courcoul et al., 2022) have measured biofilm response using classical descriptors (e.g. chlorophyll *a* content etc.) the application

of high-throughput sequencing of the *16S rRNA* gene has led to a deeper understanding of how environmental stressors and chemical pollutants affect community composition and diversity (Gionchetta et al., 2020; Lu et al., 2019; Romero et al., 2020; Rosi-Marshall et al., 2013; Timoner et al., 2014). For instance, droughts have been observed to enrich streambed biofilm bacterial communities in taxa adapted to withstand desiccation (Pohlon et al., 2013; Timoner et al., 2014). Regarding the effect of emerging contaminants (ECs), some authors have observed major alterations in bacterial community composition in response to ECs (Rosi-Marshall et al., 2013), while others reported minor effects (Lu et al., 2019). In the multiple stressors scenario, a recent study suggested that the responses of biofilm bacterial communities are hardly predictable from the effects of an individual stressor since they are modulated by interactions among stressors (Romero et al., 2020).

A useful approach that contributes to understanding the interactions of microbial populations with their environment is the analysis of the cellular phenotype (*e.g,* the complete set of proteins or metabolites i.e. proteome and metabolome), (Lips et al., 2022; Raes and Bork, 2008). Community metabolomics, for example, has been able to unravel complex biochemical changes in the periphyton during chronic and acute exposure to diuron (Lips et al., 2022). In addition, it may elucidate the metabolic pathways involved in the response to specific stress and may help propose specific stress biomarkers (Creusot et al., 2022; Serra-Compte et al., 2018). While metabolomics provides an overview of cellular metabolism, cell or system excretes (*i.e.*, the exometabolome) offer the possibility to directly characterize the molecular interaction between microbial communities and their environment. Both phototrophic and heterotrophic compartments of the biofilm exude organic compounds into the environment thus contributing to the pool of DOM (Battin et al., 2016). The biofilm microbiome is also capable of metabolising a wide range of DOM compounds, suggesting a complex and bidirectional relationship between DOM and microbial communities (Battin et al., 2016). Several studies have reported relationships between the composition of dissolved organic matter (DOM) in the

environment and bacterial activity (Fork et al., 2020; Kamjunke et al., 2019; Smith et al., 2018) contributing to a mechanistic understanding of the role of microorganisms in the global carbon cycle. The influence of stressors on interactions between microbes and DOM is poorly understood. Recent research suggests that stressors may alter interactions between dissolved organic matter and the microbial community (Romano et al., 2014; Wang et al., 2023).

Surprisingly, the application of "omics" approaches to study stressed aquatic streambed biofilms is still undeveloped. To our knowledge, there are few studies that identify the metabolic response of environmental biofilms to the impact of stressor(s) (Creusot et al., 2022; Serra-Compte et al., 2018) or provide information on DOM-microbe interactions in response to stress (Wang et al., 2023). To fill this gap, we conducted a mesocosm experiment aimed at improving our understanding of: I) how desiccation and environmentally relevant EC pollution affect the composition and metabolome of streambed biofilm bacterial communities, and II) how bacterial communities and their metabolic by-products interact with the DOM. Our case study was designed to expose streambed biofilms to a desiccation event and to assess how biofilm bacterial communities recover from this stress under polluted and non-polluted conditions. We hypothesised that the effects of stressors will be reflected in the composition of biofilm bacterial communities (both the bulk (DNA-based) and active (RNA-based) fractions), as well as metabolic and DOM profiles. W also speculated that desiccation will have more acute effects compared to EC pollution.

2. Materials and Methods

2.1. Experimental design

The experiment was performed in the indoor Experimental Streams Facility (ESF) at the Catalan Institute for Water Research (Girona, Spain) using artificial streams. General ESF operating conditions and aspects regarding biofilm colonisation are described in detail in our previous publication (Rožman et al., 2018) as well as in studies that previously used ESF (Corcoll et al., 2015; Serra-Compte et al., 2018). Overall, physical and chemical conditions in the artificial streams (water velocity, temperature, and light cycles) emulated those of the Segre River (NE Iberian Peninsula) during late spring and under low flow conditions. Experimental details are provided in the Supplementary Information (SI). The overall experimental timeline is depicted in Fig. 1. After the colonisation phase (5 weeks), the water flow was interrupted for 5 days to simulate a short dewatering period in the treatments of flow intermittency. The water content in the biofilms exposed to the dry period decreased by up to 95% at the end of the dry period, indicating that the stress was severe. Previous studies using a similar reduced/blocked flow situation of 5 to 10 days duration have shown that the stress was sufficient to induce structural and functional changes in biofilm communities comparable to those commonly found in intermittent Mediterranean streams (Corcoll et al., 2015; Serra-Compte et al., 2018; Timoner et al., 2012). Once flow was re-established, initial water and biofilm samples were taken: intermittent flow initial samples (START-IF) and continuous flow initial samples (START-CF). After the collection of the initial samples, the system underwent into the recovery phase, simulated under two scenarios: i) a pristine stream and, ii) a stream polluted with ECs. Under both scenarios we assessed how biofilm bacterial communities recover from the stress caused by flow intermittency under non-polluted and polluted conditions (combined stressors). The recovery period lasted 14 days thus allowing the evaluation of short-term recovery effects under non-polluted and polluted conditions. At the end of the recovery period final water and biofilm samples were collected: continuous flow - non EC pollution

(END-CF_noP), continuous flow-EC pollution (END-CF_P), intermittent flow - non EC pollution (END-IF_noP) and intermittent flow - EC pollution (END-IF_P), Fig. 1. Each treatment was composed of three replicated artificial streams. EC pollution was simulated using a mixture of EU watch list (EU 2015/495) substances: erythromycin, diclofenac, imidacloprid, venlafaxine and sulfisoxazole (obtained from Sigma-Aldrich, Spain). The ECs mixture was freshly prepared and administered after each water renewal. Exposure of ECs was at environmentally relevant nominal concentrations of 10^{-6} g L^{-1} for each compound. The decrease in concentrations of ECs was measured in one of our previous studies (Rožman et al., 2018). This showed that all substances used decreased by up to 10% of the measured initial concentrations after 4 days, with the exception of venlafaxine, which showed a decrease of up to 40%.

2.2. Water and biofilm sampling

Biofilm samples from all treatments and their replications were collected to carry out the characterization of biofilm bacterial communities and the analysis of the metabolome. To minimize the effects of biofilm heterogeneity, samples from each channel were obtained by pooling at least six randomly collected biofilm subsamples (0.5 ml each) along the channel streambed. For analysis of DOM, 10 mL of water was collected from all treatments and replicate channels. Although the ESF was operated with a combined scheme of open and recirculated water flow prior to collection of the DOM samples, the water flow was recirculated for at least 24 hours for the start samples and 72 hours for the final samples. Recirculation of the water flow was used to minimize the loss of DOM that would occur with open flow. After collection, all samples were stored at –80 ºC until further analysis.

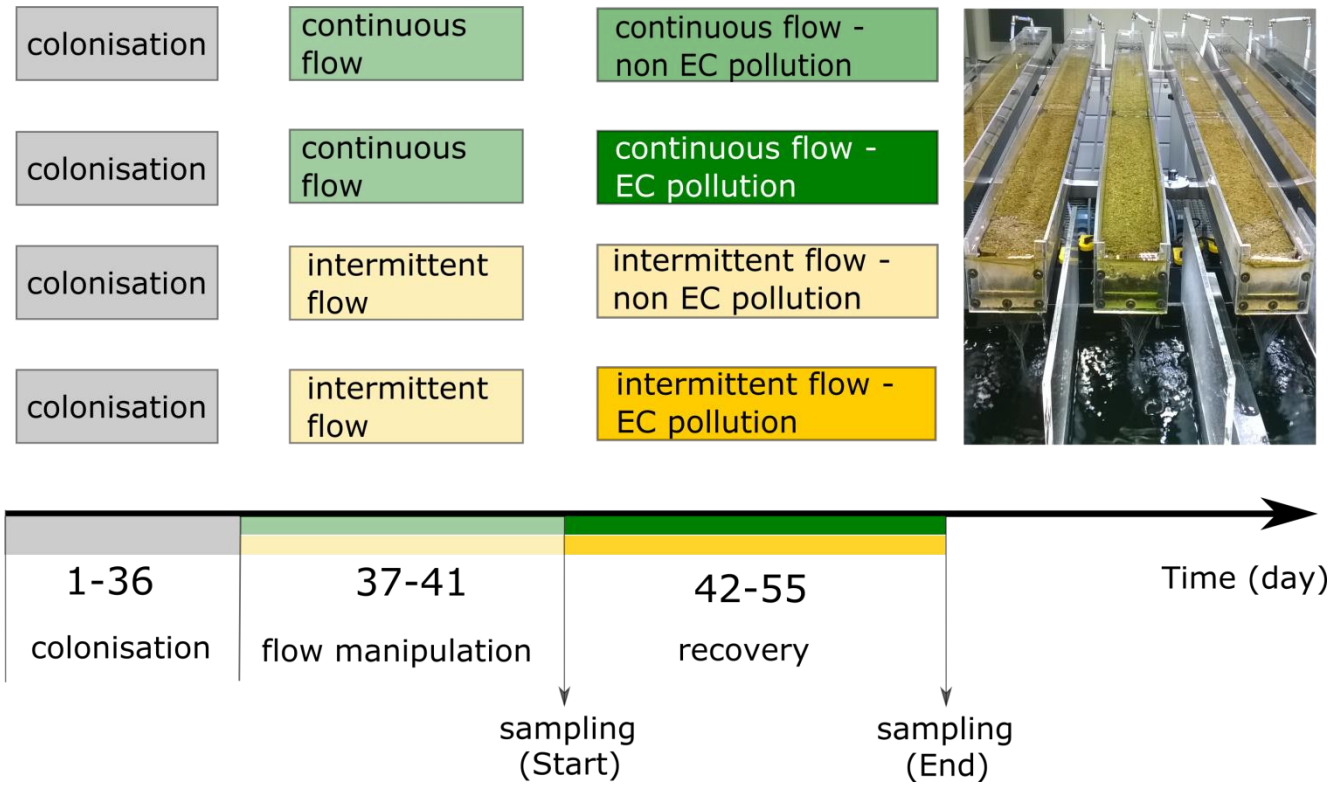

Fig. 1. Experimental design and sampling scheme used in the study.

2.3. Nucleic acid extraction, amplicon-targeted sequencing, and sequence processing.

Details on the extraction of RNA and DNA from biofilm samples, purification of resulting extracts and downstream purification procedures are described in SI. DNA and cDNA extracts were subjected to high-throughput multiplexed 16S rRNA gene sequencing with the Illumina MiSeq System (2×250 PE) using primer pair 515f/806r (Caporaso et al., 2011) complemented with Illumina adapters and sample-specific barcodes at the Research Technology Support Facility Michigan State University, USA (Kozich et al., 2013). Details on the analysis of resulting sequence datasets performed in QIIME2 2018.8 (Bolyen et al., 2019) are described in SI. The sequence dataset was deposited in the NCBI Sequence Read Archive (SRA) database under accession number PRJNA716966.

2.4. Quantification of antibiotic resistance genes (ARGs).

The pharmaceutical mixture used as treatment included two antibiotics: sulfamethoxazole (sulfonamide) and erythromycin (macrolide). We assessed the potential variation in the abundance of genes conferring resistance to these antibiotic classes, namely genes *sul1* and *sul2* (sulfonamide resistance) and *ermB* (macrolide resistance) in DNA (*i.e.*, gene copies) and RNA extracts (*i.e.*, transcript copies) obtained from biofilm bacterial communities exposed to treatments. Copy numbers of the class 1 integron-integrase gene (*intI1*) were also quantified as a proxy for anthropogenic pollution and horizontal gene transfer (Gillings et al., 2015; Stalder et al., 2014) and copy numbers of the 16S rRNA gene were quantified to normalize the concentration of all target genes. All qPCRs were run using SYBR green detection chemistry on an MX3005 system (Agilent Technologies; Santa Clara, CA, USA) as previously described (Subirats et al., 2018).

2.5. DOM and metabolite analysis

The biofilm samples were thawed on ice at 4 °C for 30–60 min, after which 0.5 ml of the biofilm sample was resuspended in 0.8 ml of ice-cold methanol/water (50:50, v/v). The metabolites were extracted on ice using an ultrasonic probe (Branson Digital sonicator, model 102C; 3 cycles of 120 s at 15 Hz of intensity). The samples were centrifuged at 14,000 × *g* for 10 min at 4 °C to pellet the protein and remove solid particles. The supernatants were collected, evaporated to dryness under a gentle nitrogen stream and reconstituted with 0.5 mL of methanol/water (50:50, v/v) before mass spectrometric analysis. DOM was solid-phase extracted from 10 ml of 0.45 µm PVDF membrane filtered (Whatman, UK) water using 60 mL Oasis HLB cartridges (Waters Corporation, USA) as described in (Previšić et al., 2020). Extracts were evaporated to dryness under a gentle nitrogen stream and reconstituted with 0.5 mL of methanol/water (50:50, v/v) before mass spectrometric analysis. Non-target analysis of the metabolome and DOM samples was performed with a high-resolution mass

spectrometry system, LTQ-Orbitrap Velos^{TM} coupled with the Aria TLX-1 HPLC system (Thermo Fisher Scientific, USA). Instrument parameters and HPLC gradients are provided in SI. Data extraction, chromatographic deconvolution and final alignment were done using the MZmine program (Katajamaa et al., 2006). The obtained data matrix was further corrected for features detected in blank samples by removing features with an intensity ratio sample:blank < 20. In the next step we removed all the features that were not present in at least two out of three replicates and the feature peak area was calculated as mean peak area of all positive values. The final data matrix was power transformed by cube root and centred. Details about the procedures and parameters regarding data extraction and features identification are provided in SI. The metabolic and DOM datasets were visualized using Van Krevelen diagrams *i.e.*, by plotting the H/C ratio against the O/C ratio (as derived from the empirical formulae) for every feature in the dataset. On the Van Krevelen map, features were classified considering density areas for the following classes of metabolites: black carbon, condensed hydrocarbon, lipids, terpenoids, flavonoids & polyketides, monosaccharides, and amino acids & peptides, as suggested in (Brockman et al., 2018). An example of empirically derived density areas is depicted in Supplementary Fig. S1. Please note that the limitation of Van Krevelen maps arises from the fact that molecules with different structures can have similar or even identical molecular formulas, thus producing an overlap of metabolite classes. Due to large number of features, Van Krevelen diagrams were used to visualize just the metabolite/DOM composition of the most important variables (i.e. the upper quartile) associated with a given principal component. Van Krevelen diagrams were created in Wolfram Mathematica technical computing program (version 10, Wolfram Research, UK) using an in-house developed script.

2.6. Data analysis and statistics. Exploratory methods were used to examine the relationships between different treatments based on the values of the measured variables. Principal coordinate

217 analysis (PCoA) was applied to the Bray Curtis distance matrix on Hellinger-transformed average of
218 amplicon sequence variants (ASV) abundance. Principal component analysis (PCA) was performed on
219 centred cube root transformed metabolite and DOM data. All exploratory analyses were done in
220 Primer 7 (Version 7.0.13, PRIMER-e, NZ). Similarity patterns between datasets (DNA and RNA
221 community, metabolome and DOM) were checked using the generalised Procrustes analysis (GPA).
222 Similarity between partial configurations was quantitatively defined by an *RV* coefficient which
223 represents square root of (1 - sum of squared differences between the two ordinations). Permutation
224 test was used to test of the significance of the Procrustes results. Procrustes analyses and permutation
225 tests were performed using procrustes and protest functions in the *vegan* R package while visualization
226 was performed using the GPA function in the *FactoMineR* R package.
227

3. Results

3.1 Effect of treatments on the composition of biofilm bacterial communities

Bacterial communities in the bulk fraction (DNA libraries) were dominated by sequences affiliated to the class Alphaproteobacteria (average relative abundance of 30.85%), Oxyphotobacteria (phylum Cyanobacteria, 20.25% on average) and, to a lesser extent, Bacteroidia (phylum Bacteroidetes, 14.85% on average) and Gammaproteobacteria (11.16% on average) (Suppl. Fig. S2A). Minor members of these communities were assigned to the classes Bacilli (Firmicutes) and Planctomycetalia (Planctomycetes). Although no significant differences in the richness (Chao1 index) and diversity (Shannon index) of bacterial communities were obtained between experimental treatments (p >0.5, data not shown), an increase in the relative abundance of Alphaproteobacteria was observed in all treatments in comparison to the beginning of the experiment (time =0) and a clear reduction in cyanobacterial sequences was also measured for treatments not subjected to desiccation (Suppl. Fig. S2A).

The composition of bacterial communities in RNA libraries (assumed as being the active fraction of communities) was similar to that observed for the bulk fraction, being dominated by sequences affiliated to Bacteroidetes, Oxyphotobacteria and Alphaproteobacteria (Suppl. Fig. S2B). However, clear differences were measured for certain bacterial groups such as members of the class Bacilli (average of 13.3% in the RNA fraction in comparison to 4.5% in the DNA fraction) and the class Planctomycetalia (average of 5.45% and 3.47% in the RNA and the DNA fractions, respectively). These variations, however, were not high enough to reach statistical significance in terms of richness and diversity (data not shown).

Ordination of samples from both bulk (DNA-based) and active (RNA-based) bacterial communities using PCoA suggested that both incubation time and treatment explained most of the variance in community composition (~64%, Fig. 2). Particularly, the first PCoA axis (~46.4% of total variance)

252 separated the initial from the final samples despite the applied treatment. The second PCoA axis
253 (~17.6% of the variance) separates samples exposed to drought from those that were not regardless of
254 their exposure to pharmaceutical compounds.

255

256 **3.2 Abundance of antibiotic resistance genes and transcripts across treatments**

257 No differences were observed when comparing the relative abundance of gene *intI1* and its transcripts
258 within the bacterial community (Suppl. Fig. S3). Regarding ARGs, the quantification of gene and
259 transcript copies of *ermB* was below the detection limit of the assay (56 copies/µL) for all samples.
260 Similarly, the quantification of *sul2* transcripts was below the limit of detection of the assay (75
261 copies/µL). Overall, the relative concentration of the *intI1* and *sul1* transcripts were approximately
262 three orders of magnitude lower than those of their corresponding genes, suggesting their low level of
263 expression under the experimental conditions assayed. Similar to the results for gene *intI1*, no
264 differences in the relative concentrations of genes *sul1* and *sul2* as well as *sul1* transcripts were
265 observed in any of the treatments.

266

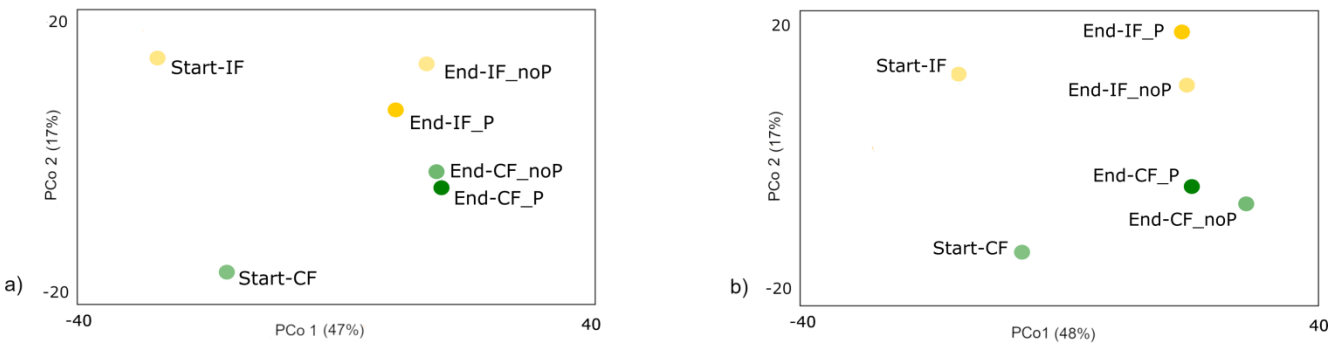

267

268 **Fig. 2.** PCoA ordination of a) bulk (DNA-based), and b) active (RNA-based) biofilm bacterial
269 communities revealed differences in their structure over incubation time and changes due to
270 desiccation.

271

3.3 Effect of treatments on the biofilm bacterial community metabolome

The bacterial community metabolome was shaped by both incubation time and environmental factors (Fig. 3a). Greater variability in metabolite profiles was observed in response to incubation time (PC1) than to desiccation (PC2), explaining 71% and 12% of the experimental variance, respectively. Metabolite features associated with variability along PC1 were mainly classified as lipids, terpenoids and polyketides on the Van Krevelen map (Fig. 3b). Activity in the lipid and terpenoid region on the Van Krevelen diagram was also related to segregation on the PC2 axis (*i.e.*, the separation between treatments with permanent and intermittent flow, Fig. 3c). In addition, the separation between treatments regarding the flow conditions was associated with distinct activity in the region of molecules that are aliphatic in structure and moderately depleted of oxygen, i.e. corresponding to the intersection between lipid and amino acids/peptides classes.

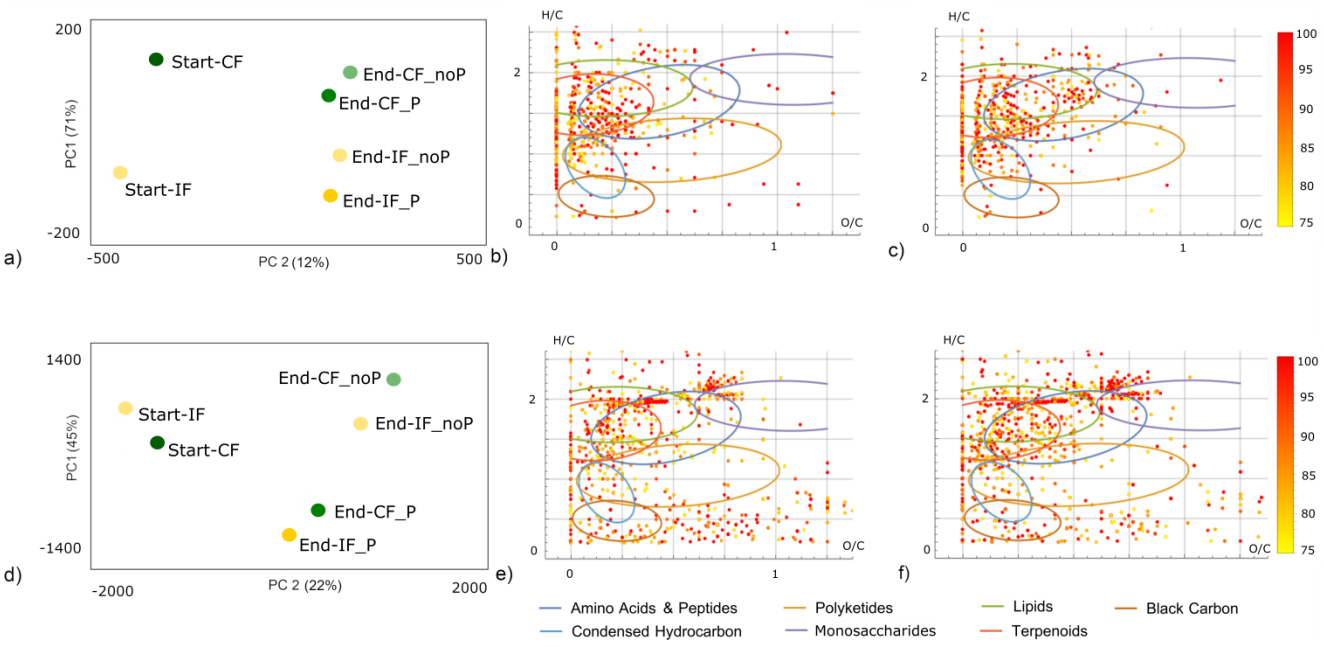

Fig. 3. Primary PC separation of a) metabolome and d) DOM experimental samples reflects incubation time discrimination of the samples. In metabolome samples, the second principal axis showed effective separation between treatments with permanent and intermittent flow, while within DOM samples, it

revealed separation between polluted and non-polluted samples collected at the end of the experiment. The most relevant metabolite (b and c) and DOM (e and f) features associated with a given PC are plotted on the Van Krevelen map. Associations are represented in a yellow-red gradient.

3.4. DOM profiles

The main driver of variation in the DOM samples was incubation time (45% of variance), suggesting a strong temporal constraint and clear distinction between samples collected at the start and the end of the experiment (Fig. 3d). Changes related to incubation time were reflected in polyketide, lipids and amino acids regions on the Van Krevelen map (Fig. 3e). The comparison of Van Krevelen diagrams for DOM and metabolome uncovered the appearance of compounds related to black carbon and condensed aromatics (Fig. 3e). The other distinct region of increased activity was the intersection between lipids, amino acids/peptides and polysaccharide classes. The second driver of variation within the DOM samples was pollution (22% of variance). It is important to stress that molecular features (if detected) related to added ECs and their possible degradation products were omitted from the analysis, thus excluding their potential influence on the DOM profile. A major region of the metabolites associated with variability between polluted and non-polluted treatments was the lipid-amino acid/peptide-polysaccharide region (Fig. 3f).

3.5. Relationship between obtained datasets

The similar performance of different datasets (*e.g.*, bulk and active community, metabolome, DOM) suggested the existence of a certain relationship between them. GPA confirmed a consistent pattern of similarity between datasets (Fig. 4 and Suppl. Table S1). Inter-omic GPA suggested that the relationship was strongest for the triad DNA–RNA–metabolome (*RV* coefficients > 0.9 and Monte Carlo *p* values < 0.05, Fig. 4). On the other hand, the DOM dataset showed weaker correlations (*RV*

coefficients ~ 0.6) and non-significant differences (Monte Carlo $p > 0.05$) with all other datasets (Fig. 4).

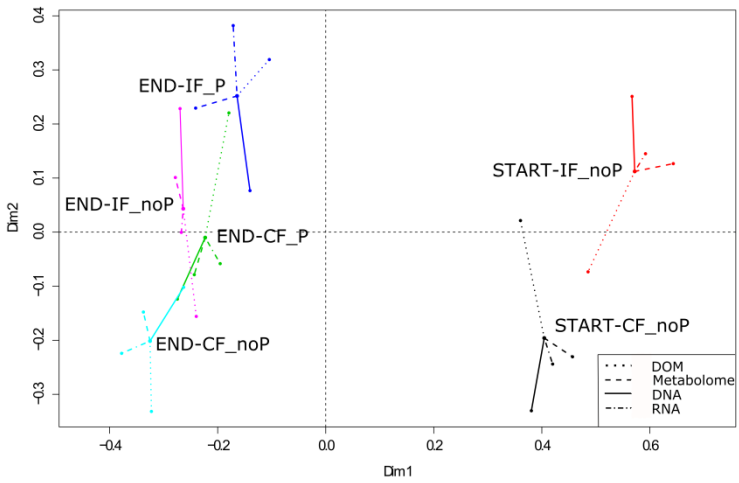

Fig. 4. a) GPA showing the proximity between distributions of the experimental samples obtained by bulk (DNA) and active (RNA) community fractions as well as metabolome and DOM datasets. Shorter lines indicate higher congruency between datasets

4. Discussion

The composition of bulk and active fractions of biofilm bacterial communities were similar to those inhabiting both experimental (Subirats et al., 2018) and natural streams (Battin et al., 2016; Timoner et al., 2014). The lack of structural responsiveness of communities to different experimental treatments was unexpected assuming the role of streambed biofilms as biosensors to gauge alterations in water quality caused by chemical pollutants (Proia et al., 2013; Sabater et al., 2007). However, analysis at lower taxonomic resolution showed that samples from bulk and active bacterial communities responded to both incubation time and desiccation. Equivalently, incubation time had a predominant influence on the community metabolome and DOM profiles. All metabolite classes of community metabolome linked to the observed temporal dynamic *i.e.*, incubation time (mainly lipids, terpenoids and polyketides, Fig. 3b) and may link to essential processes related to cell growth and biofilm formation. Both lipids and terpenoids have a key role in cell-wall biosynthesis, membrane function, and energy storage (De Carvalho and Caramujo, 2018; Tholl, 2006) while polyketides are correlated with biofilm formation (Pang et al., 2012). While it is intuitive that incubation time is reflected in the community metabolome, we should stress that DOM is produced, consumed, and altered by microbial activities, and it is expected that related changes should be reflected in the DOM. Although incubation time is equally reflected in the DOM and metabolome samples, we observed differences in the molecular classes involved. The comparison of Van Krevelen diagrams for DOM and metabolome spotted the appearance of compounds related to black carbon and condensed aromatics (Fig. 3e). Both types of compounds are refractory organic products of incomplete combustion characteristic of freshwater natural organic matter (Antony et al., 2017; Coppola et al., 2018), which were probably introduced in our experimental system through the sediment substrate used for biofilm colonization. The activity observed in this region was likely related to the microbial degradation of dissolved black carbon and condensed aromatics, as microorganisms are capable of overturning the DOM pool by

transforming these compounds (Antony et al., 2017; Hockaday et al., 2006). The other distinct region of increased activity was the intersection between lipids, amino acids/peptides and polysaccharide classes. We speculate that this region probably reflects the direct contribution of biofilm exudates, which include extracellular metabolites/enzymes, waste products, signal molecules or components of the nutrient pool exchanged between bacterial cells in the biofilm (Smith et al., 2019). Our results may therefore relate to normal biofilm growth and maturation and the associated excretion of a diverse array of compounds.

So far, our results revealed a significant inter-omic structure, indicating that the composition of bacterial communities (both active and bulk fractions) is consistent with endogenous and exogenous metabolites. However, we found that desiccation shaped the biofilm metabolome and the composition of biofilm bacterial communities, while EC pollution did not affect biofilm recovery. On the other hand, EC pollution shaped the chemical composition of the flowing water, while desiccation did not induce any observable variation in DOM composition. Although the results support our initial hypothesis that the stressor effects will be reflected in different "-omics" datasets, the question regarding why EC pollution-induced stress was observable in the DOM but not in the metabolome dataset remains. Subsequently, we attempted to explain the nature of these observations. The molecular mechanisms behind maintaining cytoplasmic hydration may explain why the metabolome samples showed variability associated with desiccation, in contrast to DOM samples. To overcome osmotic stress, bacteria can either acquire or synthesize osmoprotectants (Meadows and Wargo, 2015; Wood et al., 2001). Osmoprotectants are usually electrolytes (*e.g.*, K^+) or, more often, carboxylic acid derivatives, amino acids and their derivatives. Distinct activity at the intersection between lipid and amino acids/peptides region (Fig. 3c) corresponded to profiles of carboxylic acid derivatives such as carnitine, acetylcarnitine and azelaic acid. Carnitine and acetylcarnitine are used by bacteria as osmoprotectants and/or osmolytes (Meadows and Wargo, 2015) while azelaic acid has been attributed to desiccation stress (Serra-Compte et al., 2018). Changes in amino acid/peptide levels as a result of

desiccation could be related to their role as osmoprotectants (Kol et al., 2010). In our experiment, the desiccation event lasted for 5 days, during which biofilm (as a whole) tried to maintain its overall physiological status, preserving both cellular viability and hydration. Due to the duration of the stress event, however, cells probably triggered stress-response mechanisms that contributed to the observed differences between metabolome samples. Upon rehydration and osmotic downshock, some osmoprotectants were rapidly released into their environment, most likely contributing to the desiccation "signature" in DOM. However, we were unable to detect this response since the time frame of these releases is likely much faster (<60 s according to (Wood et al., 2001)) than the resolution of our measurement. On the other hand, the majority of osmoprotectants are usually fully retained by the cells (Wood et al., 2001), thus probably contributing to a desiccation signature of biofilm cells.

Metabolome samples did not exhibit differences depending on exposure to contaminants due to relatively low concentrations of ECs, which neither significantly altered the composition of bulk and active fractions of biofilm bacterial communities nor caused any up- or down-regulation in ARG expression. This result agrees with a previous study where streambed bacterial communities were subjected to a combined regime of nutrients and emerging contaminants (Subirats et al., 2018), and where significant differences in ARG abundance were only measured for communities exposed to both chemical pollutants and high nutrient concentrations. A recent study found that similar concentrations of antibiotics administered to an aquatic microbial community did not impact gene expression related to replication, transcription, translation, and cell growth (Lu et al., 2019). This implies that the concentrations of ECs used in our experiment were too low to significantly impact the short-term recovery of streambed microbiota and their metabolome, making desiccation a more severe stressor than chemical pollution. This is also consistent with previous studies reporting desiccation as the dominant factor when both desiccation and pharmaceuticals acted as stressors (Serra-Compte et al., 2018). Given our incomplete understanding of biofilm exudates, the issue of why DOM samples

reflect EC pollution cannot be fully resolved. We can only point out that our results are consistent with the recent hypothesis that bacteria excrete certain compounds under EC stress (Lu et al., 2019). This hypothesis is supported by the fact that many bacteria secrete extracellular enzymes to degrade complex polysaccharides and proteins (Smith et al., 2019), suggesting that biofilm response to EC pollution is mainly extracellular. It is also worth mentioning that despite the fact that some processes linked to pollution may be noticed at the metabolome level (Booth et al., 2011; Previšić et al., 2020), their biomarkers probably remained hidden under the acute effects caused by desiccation.

In conclusion, our results demonstrate a dynamic interaction between microbial biofilm and its environment. Incubation time and desiccation stress defined the biofilm community and its metabolome. In contrast, biofilm recovery under EC pollution at environmentally relevant concentrations affected neither the biofilm microbial community nor its metabolome. However, the microbial biofilm under the impact of EC pollution changed the chemical composition of DOM, while no evidence of desiccation stress was found. Metabolome profiling suggests that the intracellular response to desiccation may be related to mechanisms associated with oxidative stress and maintenance of cytoplasmic hydration. On the other hand, the composition of DOM suggests that the bacterial community may excrete certain compounds in response to EC stress. This study suggests that, for fluvial biofilm, many genotype-to-phenotype relationships exist which is a first step towards gaining mechanistic insights into how organisms respond to stress. In a next step, we aim to elucidate the key functional capabilities of the major taxa to understand the complex network of interactions at different molecular levels that contribute to community functioning and the composition of biologically produced DOM.

Acknowledgements

We thank Vicenç Acuña and Maria Casellas (ICRA, Spain) for their help with the implementation of the study design at the Experimental Streams Facility. Proofreading by Katarina Cetinić (Ruđer Bošković Institute, Zagreb) is gratefully acknowledged. This work has been supported by the European Union's Horizon 2020 research and innovation programme under the Marie Sklodowska-Curie grant agreement No. 657425 - TRANSFORMER project and by the Croatian Science Foundation project no. IP-2018-01-2298. ICRA authors acknowledge the European Regional Development Found (FEDER) and the Generalitat de Catalunya through the Consolidated Research Group (SGR ICRA-ENV 2021 01282) and the funding from the CERCA program.

Competing Interests:

The authors declare that they have no known competing financial interests or personal relationships that could have appeared to influence the work reported in this paper.

Data availability

The sequence dataset was deposited in the NCBI Sequence Read Archive (SRA) database under accession number PRJNA716966. All scripts used in this work, as well as other data that support the findings of this study are available on reasonable request from the corresponding author.

References

Antony, R., Willoughby, A.S., Grannas, A.M., Catanzano, V., Sleighter, R.L., Thamban, M., Hatcher, P.G., Nair, S., 2017. Molecular Insights on Dissolved Organic Matter Transformation by Supraglacial Microbial Communities. Environ. Sci. Technol. 51, 4328–4337. https://doi.org/10.1021/acs.est.6b05780

Battin, T.J., Besemer, K., Bengtsson, M.M., Romani, A.M., Packmann, A.I., 2016. The ecology and biogeochemistry of stream biofilms. Nat. Rev. Microbiol. 14, 251–263. https://doi.org/10.1038/nrmicro.2016.15

Bolyen, E., Rideout, J.R., Dillon, M.R., Bokulich, N.A., Abnet, C.C., Al-Ghalith, G.A., Alexander, H., Alm, E.J., Arumugam, M., Asnicar, F., Bai, Y., Bisanz, J.E., Bittinger, K., Brejnrod, A., Brislawn, C.J., Brown, C.T., Callahan, B.J., Caraballo-Rodríguez, A.M., Chase, J., Cope, E.K., Da Silva, R., Diener, C., Dorrestein, P.C., Douglas, G.M., Durall, D.M., Duvallet, C., Edwardson, C.F., Ernst, M., Estaki, M., Fouquier, J., Gauglitz, J.M., Gibbons, S.M., Gibson, D.L., Gonzalez, A., Gorlick, K., Guo, J., Hillmann, B., Holmes, S., Holste, H., Huttenhower, C., Huttley, G.A., Janssen, S., Jarmusch, A.K., Jiang, L., Kaehler, B.D., Kang, K. Bin, Keefe, C.R., Keim, P., Kelley, S.T., Knights, D., Koester, I., Kosciolek, T., Kreps, J., Langille, M.G.I., Lee, J., Ley, R., Liu, Y.X., Loftfield, E., Lozupone, C., Maher, M., Marotz, C., Martin, B.D., McDonald, D., McIver, L.J., Melnik, A. V., Metcalf, J.L., Morgan, S.C., Morton, J.T., Naimey, A.T., Navas-Molina, J.A., Nothias, L.F., Orchanian, S.B., Pearson, T., Peoples, S.L., Petras, D., Preuss, M.L., Pruesse, E., Rasmussen, L.B., Rivers, A., Robeson, M.S., Rosenthal, P., Segata, N., Shaffer, M., Shiffer, A., Sinha, R., Song, S.J., Spear, J.R., Swafford, A.D., Thompson, L.R., Torres, P.J., Trinh, P., Tripathi, A., Turnbaugh, P.J., Ul-Hasan, S., van der Hooft, J.J.J., Vargas, F., Vázquez-Baeza, Y., Vogtmann, E., von Hippel, M., Walters, W., Wan, Y., Wang, M., Warren, J., Weber, K.C., Williamson, C.H.D., Willis, A.D., Xu, Z.Z., Zaneveld, J.R., Zhang, Y., Zhu, Q., Knight, R., Caporaso, J.G., 2019. Reproducible, interactive, scalable and extensible microbiome data science using QIIME 2. Nat. Biotechnol. 37, 852–857. https://doi.org/10.1038/s41587-019-0209-9

Booth, S.C., Workentine, M.L., Wen, J., Shaykhutdinov, R., Vogel, H.J., Ceri, H., Turner, R.J., Weljie, A.M., 2011. Differences in metabolism between the biofilm and planktonic response to metal stress. J. Proteome Res. 10, 3190–3199. https://doi.org/10.1021/pr2002353

Brockman, S.A., Roden, E. V., Hegeman, A.D., 2018. Van Krevelen diagram visualization of high resolution-mass spectrometry metabolomics data with OpenVanKrevelen. Metabolomics 14, 1–5. https://doi.org/10.1007/s11306-018-1343-y

Calapez, A.R., Elias, C.L., Alves, A., Almeida, S.F.P., Brito, A.G., Feio, M.J., 2020. Shifts in biofilms' composition induced by flow stagnation, sewage contamination and grazing. Ecol. Indic. 111, 106006. https://doi.org/10.1016/j.ecolind.2019.106006

Caporaso, J.G., Lauber, C.L., Walters, W.A., Berg-Lyons, D., Lozupone, C.A., Turnbaugh, P.J., Fierer, N., Knight, R., 2011. Global patterns of 16S rRNA diversity at a depth of millions of sequences per sample. Proc. Natl. Acad. Sci. U. S. A. 108, 4516–4522. https://doi.org/10.1073/pnas.1000080107

Coppola, A.I., Wiedemeier, D.B., Galy, V., Haghipour, N., Hanke, U.M., Nascimento, G.S., Usman, M., Blattmann, T.M., Reisser, M., Freymond, C. V., Zhao, M., Voss, B., Wacker, L., Schefuß, E., Peucker-Ehrenbrink, B., Abiven, S., Schmidt, M.W.I., Eglinton, T.I., 2018. Global-scale evidence

for the refractory nature of riverine black carbon. Nat. Geosci. 11, 584–588. https://doi.org/10.1038/s41561-018-0159-8

Corcoll, N., Casellas, M., Huerta, B., Guasch, H., Acuña, V., Rodríguez-Mozaz, S., Serra-Compte, A., Barceló, D., Sabater, S., 2015. Effects of flow intermittency and pharmaceutical exposure on the structure and metabolism of stream biofilms. Sci. Total Environ. 503–504, 159–170. https://doi.org/10.1016/j.scitotenv.2014.06.093

Courcoul, C., Leflaive, J., Ferriol, J., Boulêtreau, S., 2022. The sensitivity of aquatic microbial communities to a complex agricultural contaminant depends on previous drought conditions. Water Res. 217. https://doi.org/10.1016/j.watres.2022.118396

Creusot, N., Chaumet, B., Eon, M., Mazzella, N., Moreira, A., Morin, S., 2022. Metabolomics insight into the influence of environmental factors in responses of freshwater biofilms to the model herbicide diuron. Environ. Sci. Pollut. Res. 29, 29332–29347. https://doi.org/10.1007/s11356-021-17072-7

De Carvalho, C.C.C.R., Caramujo, M.J., 2018. The various roles of fatty acids. Molecules 23. https://doi.org/10.3390/molecules23102583

Fork, M.L., Osburn, C.L., Heffernan, J.B., 2020. Bioavailability and compositional changes of dissolved organic matter in urban headwaters. Aquat. Sci. 82, 1–15. https://doi.org/10.1007/s00027-020-00739-7

Gillings, M.R., Gaze, W.H., Pruden, A., Smalla, K., Tiedje, J.M., Zhu, Y.G., 2015. Using the class 1 integron-integrase gene as a proxy for anthropogenic pollution. ISME J. 9, 1269–1279. https://doi.org/10.1038/ismej.2014.226

Gionchetta, G., Artigas, J., Arias-Real, R., Oliva, F., Romaní, A.M., 2020. Multi-model assessment of hydrological and environmental impacts on streambed microbes in Mediterranean catchments. Environ. Microbiol. 22, 2213–2229. https://doi.org/10.1111/1462-2920.14990

Grgić, I., Cetinić, K.A., Karačić, Z., Previšić, A., Rožman, M., 2023. Fate and effects of microplastics in combination with pharmaceuticals and endocrine disruptors in freshwaters: Insights from a microcosm experiment. Sci. Total Environ. 859. https://doi.org/10.1016/j.scitotenv.2022.160387

Hockaday, W.C., Grannas, A.M., Kim, S., Hatcher, P.G., 2006. Direct molecular evidence for the degradation and mobility of black carbon in soils from ultrahigh-resolution mass spectral analysis of dissolved organic matter from a fire-impacted forest soil. Org. Geochem. 37, 501–510. https://doi.org/10.1016/j.orggeochem.2005.11.003

Kamjunke, N., Hertkorn, N., Harir, M., Schmitt-Kopplin, P., Griebler, C., Brauns, M., von Tümpling, W., Weitere, M., Herzsprung, P., 2019. Molecular change of dissolved organic matter and patterns of bacterial activity in a stream along a land-use gradient. Water Res. 164, 114919. https://doi.org/10.1016/j.watres.2019.114919

Katajamaa, M., Miettinen, J., Orešič, M., 2006. MZmine: Toolbox for processing and visualization of mass spectrometry based molecular profile data. Bioinformatics 22, 634–636. https://doi.org/10.1093/bioinformatics/btk039

Keller, V.D.J., Williams, R.J., Lofthouse, C., Johnson, A.C., 2014. Worldwide estimation of river concentrations of any chemical originating from sewage-treatment plants using dilution factors.

517 Environ. Toxicol. Chem. 33, 447–452. https://doi.org/10.1002/etc.2441

518 Kol, S., Elena Merlo, M., Scheltema, R.A., De Vries, M., Vonk, R.J., Kikkert, N.A., Dijkhuizen, L.,
519 Breitling, R., Takano, E., 2010. Metabolomic characterization of the salt stress response in
520 streptomyces coelicolor. Appl. Environ. Microbiol. 76, 2574–2581.
521 https://doi.org/10.1128/AEM.01992-09

522 Kozich, J.J., Westcott, S.L., Baxter, N.T., Highlander, S.K., Schloss, P.D., 2013. Development of a
523 dual-index sequencing strategy and curation pipeline for analyzing amplicon sequence data on the
524 miseq illumina sequencing platform. Appl. Environ. Microbiol. 79, 5112–5120.
525 https://doi.org/10.1128/AEM.01043-13

526 Lips, S., Larras, F., Schmitt-Jansen, M., 2022. Community metabolomics provides insights into
527 mechanisms of pollution-induced community tolerance of periphyton. Sci. Total Environ. 824,
528 153777. https://doi.org/10.1016/j.scitotenv.2022.153777

529 Lu, T., Zhu, Y., Ke, M., Peijnenburg, W.J.G.M., Zhang, M., Wang, T., Chen, J., Qian, H., 2019.
530 Evaluation of the taxonomic and functional variation of freshwater plankton communities induced
531 by trace amounts of the antibiotic ciprofloxacin. Environ. Int. 126, 268–278.
532 https://doi.org/10.1016/j.envint.2019.02.050

533 Meadows, J.A., Wargo, M.J., 2015. Carnitine in bacterial physiology and metabolism. Microbiol.
534 (United Kingdom) 161, 1161–1174. https://doi.org/10.1099/mic.0.000080

535 Murray, K.E., Thomas, S.M., Bodour, A.A., 2010. Prioritizing research for trace pollutants and
536 emerging contaminants in the freshwater environment. Environ. Pollut. 158, 3462–3471.
537 https://doi.org/10.1016/j.envpol.2010.08.009

538 Pang, J.M., Layre, E., Sweet, L., Sherrid, A., Moody, D.B., Ojha, A., Sherman, D.R., 2012. The
539 polyketide pks1 contributes to biofilm formation in Mycobacterium tuberculosis. J. Bacteriol.
540 194, 715–721. https://doi.org/10.1128/JB.06304-11

541 Pohlon, E., Fandino, A.O., Marxsen, J., 2013. Bacterial community composition and extracellular
542 enzyme activity in temperate streambed sediment during drying and rewetting. PLoS One 8.
543 https://doi.org/10.1371/journal.pone.0083365

544 Previšić, A., Rožman, M., Mor, J.R., Acuña, V., Serra-Compte, A., Petrović, M., Sabater, S., 2020.
545 Aquatic macroinvertebrates under stress: Bioaccumulation of emerging contaminants and
546 metabolomics implications. Sci. Total Environ. 704, 13533.
547 https://doi.org/10.1016/j.scitotenv.2019.135333

548 Proia, L., Vilches, C., Boninneau, C., Kantiani, L., Farré, M., Romaní, A.M., Sabater, S., Guasch, H.,
549 2013. Drought episode modulates the response of river biofilms to triclosan. Aquat. Toxicol. 127,
550 36–45. https://doi.org/10.1016/j.aquatox.2012.01.006

551 Raes, J., Bork, P., 2008. Molecular eco-systems biology: towards an understanding of community
552 function. Nat. Rev. Microbiol. 6, 693–699. https://doi.org/10.1038/nrmicro1935

553 Romano, S., Dittmar, T., Bondarev, V., Weber, R.J.M., Viant, M.R., Schulz-Vogt, H.N., 2014. Exo-
554 metabolome of Pseudovibrio sp. FO-BEG1 analyzed by ultra-high resolution mass spectrometry
555 and the effect of phosphate limitation. PLoS One 9. https://doi.org/10.1371/journal.pone.0096038

556 Romero, F., Acuña, V., Sabater, S., 2020. Multiple stressors determine community structure and

estimated function of river biofilm bacteria. Appl. Environ. Microbiol. 86, 1–13. https://doi.org/10.1128/AEM.00291-20

Rosi-Marshall, E.J., Kincaid, D.W., Bechtold, H.A., Royer, T. V., Rojas, M., Kelly, J.J., 2013. Pharmaceuticals suppress algal growth and microbial respiration and alter bacterial communities in stream biofilms. Ecol. Appl. 23, 583–593. https://doi.org/10.1890/12-0491.1

Rožman, M., Acuña, V., Petrović, M., 2018. Effects of chronic pollution and water flow intermittency on stream biofilms biodegradation capacity. Environ. Pollut. 233, 1131–1137. https://doi.org/10.1016/j.envpol.2017.10.019

Sabater, S., Guasch, H., Ricart, M., Romaní, A., Vidal, G., Klünder, C., Schmitt-Jansen, M., 2007. Monitoring the effect of chemicals on biological communities. the biofilm as an interface. Anal. Bioanal. Chem. 387, 1425–1434. https://doi.org/10.1007/s00216-006-1051-8

Sabater, S., Timoner, X., Borrego, C., Acuña, V., 2016. Stream biofilm responses to flow intermittency: From cells to ecosystems. Front. Environ. Sci. 4, 1–10. https://doi.org/10.3389/fenvs.2016.00014

Serra-Compte, A., Corcoll, N., Huerta, B., Rodríguez-Mozaz, S., Sabater, S., Barceló, D., Álvarez-Muñoz, D., 2018. Fluvial biofilms exposed to desiccation and pharmaceutical pollution: New insights using metabolomics. Sci. Total Environ. 618, 1382–1388. https://doi.org/10.1016/j.scitotenv.2017.09.258

Smith, H.J., Dieser, M., Mcknight, D.M., Sanclements, M.D., Foreman, C.M., 2018. Relationship between dissolved organic matter quality and microbial community composition across polar glacial environments 1–10. https://doi.org/10.1093/femsec/fiy090

Smith, N.W., Shorten, P.R., Altermann, E., Roy, N.C., McNabb, W.C., 2019. The Classification and Evolution of Bacterial Cross-Feeding. Front. Ecol. Evol. 7, 1–15. https://doi.org/10.3389/fevo.2019.00153

Stalder, T., Barraud, O., Jové, T., Casellas, M., Gaschet, M., Dagot, C., Ploy, M.C., 2014. Quantitative and qualitative impact of hospital effluent on dissemination of the integron pool. ISME J. 8, 768–777. https://doi.org/10.1038/ismej.2013.189

Subirats, J., Timoner, X., Sànchez-Melsió, A., Balcázar, J.L., Acuña, V., Sabater, S., Borrego, C.M., 2018. Emerging contaminants and nutrients synergistically affect the spread of class 1 integron-integrase (intI1) and sul1 genes within stable streambed bacterial communities. Water Res. 138, 77–85. https://doi.org/10.1016/j.watres.2018.03.025

Tholl, D., 2006. Terpene synthases and the regulation, diversity and biological roles of terpene metabolism. Curr. Opin. Plant Biol. 9, 297–304. https://doi.org/10.1016/j.pbi.2006.03.014

Timoner, X., Acuña, V., Von Schiller, D., Sabater, S., 2012. Functional responses of stream biofilms to flow cessation, desiccation and rewetting. Freshw. Biol. 57, 1565–1578. https://doi.org/10.1111/j.1365-2427.2012.02818.x

Timoner, X., Borrego, C.M., Acuña, V., Sabater, S., 2014. The dynamics of biofilm bacterial communities is driven by flow wax and wane in a temporary stream. Limnol. Oceanogr. 59, 2057–2067. https://doi.org/10.4319/lo.2014.59.6.2057

Veseli, M., Rožman, M., Vilenica, M., Petrović, M., Previšić, A., 2022. Bioaccumulation and

bioamplification of pharmaceuticals and endocrine disruptors in aquatic insects. Sci. Total Environ. 838. https://doi.org/10.1016/j.scitotenv.2022.156208

Wang, Z., Hu, X., Kang, W., Qu, Q., Feng, R., Mu, L., 2023. Interactions between dissolved organic matter and the microbial community are modified by microplastics and heat waves. J. Hazard. Mater. 448, 130868. https://doi.org/10.1016/j.jhazmat.2023.130868

Wood, J.M., Bremer, E., Csonka, L.N., Kraemer, R., Poolman, B., Van der Heide, T., Smith, L.T., 2001. Osmosensing and osmoregulatory compatible solute accumulation by bacteria. Comp. Biochem. Physiol. - A Mol. Integr. Physiol. 130, 437–460. https://doi.org/10.1016/S1095-6433(01)00442-1